Journal of Medicinal and Nanomaterials Chemistry 3 (2020) 167-188

SPC

Journal of Medicinal and Nanomaterials Chemistry

Journal homepage: https://jmnc.samipubco.com/

Orginal Research Article

Eco-friendly 2,4-D dimethylamine herbicide delivery system using synthesized nano-matrix

Itodo Ugbede Happiness[a,*], Raymond Wuana[b], Nnamonu Lami[b], Sha'ato Rufus[b]

[a] *Department of Chemistry, Federal University of Science and Technology, P.M.B. 2373 Makurdi, Nigeria*

[b] *Department of Chemistry, Federal University of Agriculture, P.M.B. 2373 Makurdi, Nigeria*

ARTICLE INFORMATION

Received: ٨ November 2019
Received in revised: 2 January 2020
Accepted: 6 January 2020
Available online: 11 April 2020

DOI: 10.48309/JMNC.2020.3.2

KEYWORDS

Green synthesis
Herbicidal delivery
Encapsulation
Soil

ABSTRACT

This study used chitosan as a capping agent and L-ascorbic acid as reducing agent to prepare copper nanoparticles encapsulated with 2,4-D dimethylamine herbicide *via* a green chemical reduction method to improve its herbicidal activity and reduce the negative environmental impacts associated with its application. Characterization of the synthesized CuCtsNPs and 2,4-D-CuCtsNPs was carried out using the following techniques; transmission electron microscopy (TEM), fourier transform- infra-red (FT-IR), scanning electron microscopy (SEM), energy-dispersive x-ray (EDX), powder x-ray diffraction (PXRD), differential scanning calorimeter (DSC), thermogravimetric and differential thermal analysis (TGA/DTA). The maximum absorption peak of CuCtsNPs was observed around 560 nm while that of 2,4-D-CuCtsNPs at 558 nm. The yield of CuCtsNPs was at the range of 40-92% and encapsulation efficiency of the 2,4-D-CuCtsNPs formulationwas 93%. Debye- Scherer's equation was used to calculate the average crystalline size of the synthesized CuCtsNPs and 2,4-D-CuCtsNPs. The values were 38.78 nm (CuCtsNPs) and 54.93 nm (2,4-D-CuCtsNPs) respectively. The SEM images revealed the particle size of 21-56 nm for CuCtsNPs and 25-69 nm for 2,4-D-CuCtsNPs. The results obtained from the DSC and TGA curves of CuCtsNPs and 2,4-D-CuCtsNPs showed that the formulations exist in crystalline state and were thermally stable up to 401.73 °C. Aqueous release studies for the formulation were carried out in three different pH media and two agricultural soils. Leaching profile of the loaded CuCtsNPs through the soil layer (UAM and CAPS) demonstrated that the UAM soil had higher value for 2,4-D (58.67%) than in CAPS soil 40.78%. This study formulated an environmentally friendly herbicide delivery nano-matrix (CuCtsNPs) for the successful slow release of 2,4-D Dimethylamine herbicide in aqueous medium and agricultural soils.

Corresponding author, email: itodohu@gmail.com (I.U. Happiness).
Tel.: +2348053695331.

Graphical Abstract

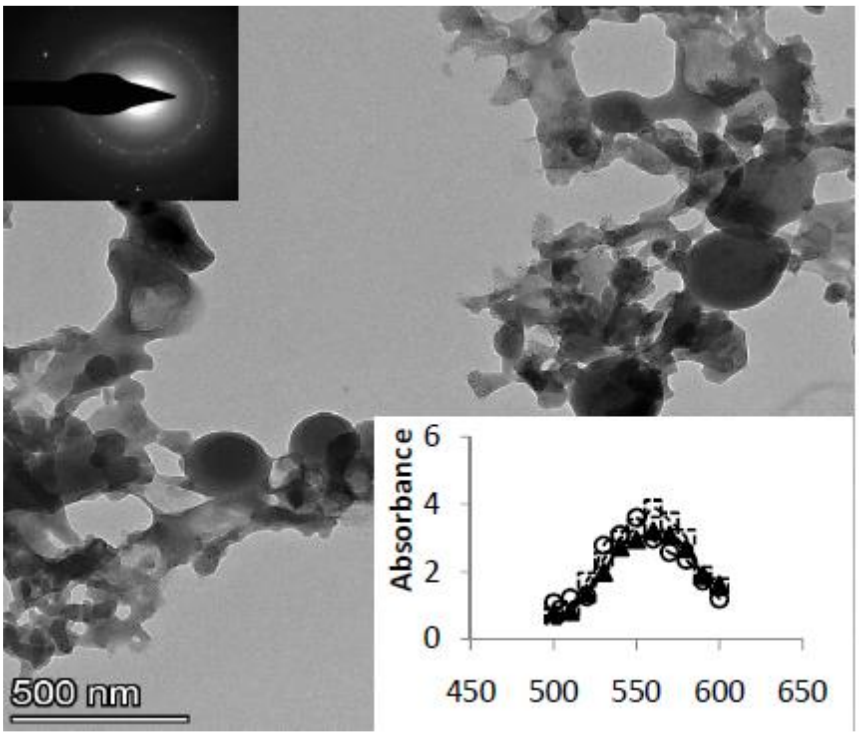

Introduction

The presence and continuous growth of weeds on the cultivated farmlands is a major factor in decreased agricultural food production thereby posing serious challenge on food security. Plants form the world's primary food source both for man and animal and the rapid growth in human population in recent years made it a necessity to maximize agricultural yields to meet the world's food demand [1]. To increase agricultural yields so as to provide adequate food for the global population, estimated by population bureau to have reached 7.5 billion [4], there is need to control weeds. Weeds are known as the hidden enemies of crops and one of the major causes of low crop yield as they compete with desired crops for nutrients [2, 3]. Nigeria, one of the most populated parts of the world has the population of about 191 million people by estimation all need food to survive and if the population is not controlled, it is expected to rise to about 411 million by 2050 that is, 2.15 times of the present population [4]. Agricultural practices associated with green revolution have greatly increased global food supply. However, impact from the excessive, inappropriate, and uncontrolled use of farm-inputs especially synthetic agrochemicals, fertilizers and heavy agricultural machinery for plant growth and protection cannot be overemphasized [5, 6]. This have led to increased resistance in plant pathogenic microbes, negative impact on non-target organisms, deterioration of soil health, increased level of toxins in the soils, groundwater and surface waters which are threatening to life and life supporting systems thereby placing the earth under serious threat [7, 8].

To combat these environmental challenges, potential emphasis needs to be concentrated on developing an effective and more

environmentally or eco-friendly pesticide delivery system with proper active ingredients that are biodegradable based, for effective and safer application for crops protection as sustainable agriculture has become a matter of concern in the development agenda [9, 10]. Several technologies have been proposed in order to minimize the spread of agrochemicals in the environment, among which are nano- and micro-particulate systems which is designed to provide controlled or sustainable release of such classes of compounds in agriculture [11, 12, 1].

2,4-Dichlorophenoxyacetic acid, more commonly referred to as 2,4-D, is one of the most widely used herbicides. 2,4-D formulation is chemically known as 2, 4-dichlorophenoxyacetic acid (2-hydroxyethyl) trimethylammonium salt [13]. It is a selective systemic herbicide used to control broadleaf weeds and was one of the first synthetic auxin herbicides to be widely and commonly used to control annual and perennial weeds [14]. The continuous usage of 2,4-D products as the most commonly employed herbicides in the world today is owned to its low cost. There are over 600 2,4-D products currently in the market. It effectively controls unwanted and invasive weeds across agricultural fields, lawns, public parks, lakes and more [14]. It is capable of causing plant injuries and damages such as stem and petiole twisting, leaf malformations, stunt root growth for broadleaf plant while rolled leaves, fused brace roots, leaning stems and stalk brittleness for grass plants [15]. Its formulations are designed to play the same role as natural auxin, indole-3-yl-acetic acid which vital in the division, differentiation and elongation of plant cells and they can naturally disrupt plant growth [14, 16]. The herbicide is non-volatile and soluble in water [16]. When applied to dicotyledonous plants at effective doses, 2,4-D is absorbed through roots, stems, and leaves, and is then translocated to the meristems of the plant [17] and in the process, uncontrolled and unsustainable growth follows, causing stem curl-over, leaf withering, and eventual plant death [18]. Several forms of 2,4-D will degrade rapidly to form 2,4-D acid under most environmental conditions. Its amine salts and esters are not persistent because of its relatively short half-life. 2,4-D show low persistence in both soil and water. It is highly mobile as it does not bind with minerals in soils and as a result has a high potential to leach from soils. 2,4-D is less likely to contami-nate groundwater due to its rapid degrada-tion [15, 19, 14, 20, 21].

Nanotechnology is gaining increased attention as a way of improving the effectiveness of herbicides and also minimizes their impacts on the environment at the same time [22]. Nanotechnological potentials are exploited for the formulation of nanoherbicides for the effective delivery of herbicides' active ingredient to the desired target using nanomaterials-based herbicide formulations [23]. Encapsulation of active ingredient within a controlled release system helps in maintaining the level at which the release process is achieved thereby prolonging the protection of the seedling until it is physically strong enough to withstand any attack. Micro or nanoencapsulation of the active ingredient provides numerous possibilities in obtaining an efficient and economically beneficial pest control and management system [11, 24, 25].

Among the numerous methods used for metal nanoparticle synthesis, chemical reduction method is one of the most convenient methods employed for synthesizing metallic nanoparticles as this synthetic process is simple, while the shape and size of nanoparticles generated can be controlled [26]. Copper nanoparticles among other metals have again much attention because of their catalytic

and optical properties and also high electrical and heat conductivity [27]. Green synthesis of copper nanoparticles is of great interest because of its many advantages. It is cheaper than silver and gold which made it an excellent material for nanoparticle. However, aggregation and oxidation are the main problems associated with copper nanoparticles. These problems can be overcome by selecting suitable stabilizer for the capping of copper nanoparticles [28].

Researches carried out by several authors established that the use carrier systems for herbicide delivery provide better weed control without negative effect on non-target organisms. Among the various nanostructured systems that can be used with herbicides, some of the most promising are based on polymeric materials [29, 30]. One polymer that has gained effective use in the area of agriculture is chitosan, a biodegradable substance obtained from the deacetylation of chitin. It is highly effective as a carrier system for the delivery of agrochemicals and plant micronutrients [31, 22]. Chitosan is a natural product derived from chitin, a polysaccharide foundation in the exoskeletons of shellfish like shrimps and crabs, a versatile biomaterial [32, 33, 34]. The ability of chitosan to chelate metals made it useful as a good stabilizer for Cu-NPs due to its biocompatibility, biodegradability, high permeability, cost-effectiveness, non-toxicity and excellent film forming ability [31, 35]. In this present study, the simple, effective and direct synthesis, characterization and slow release of 2,4-D from copper-chitosan nanoparticles (CuCtsNPs) was reported. The encapsulation of 2,4-D herbicide onto CuCtsNPs was characterized using TEM,SEM, FT-IR, XRD, DSC, TGA/DTA and EDX techniques. The slow release experiment of 2,4-D from CuCtsNPs in water, three pH media and two agricultural soils was monitored using UV-Visible spectrophotometer.

Experimental

Materials and methods

All the chemicals procured for this study were used without further purification. High molecular weight chitosan and analytical grade of 2,4-D PESTANAL® (99.9%) were supplied by Sigma Aldrich, Germany. Commercial formulation of 2,4-D with trade name Amminoforce® was supplied by Anhui Zhongshan chemicals China. Other includes; $CuSO_4.5H_2O$, L-ascorbic acid, Acetic acid (99.5%), $CaCl_2$, NaOH and distilled water. The release media pH of 5.5, 7.0 and 8.0 buffers were prepared from potassium hydrogen phthalate, potassium dihydrogen orthophosphate, NaOH and HCl. All the solutions were prepared using distilled water. Characterizations were carried out using the UV-Visible spectrophotometer (Cary 300), TEM (HRTEM, TF 20 Tecnai G^2 200 kV FEI), SEM (Tescan SEM VEGA3), Fourier transform infrared (FT-IR), X-ray diffraction (XRD), differential scanning calorimetry (DSC) spectroscopy, thermogravimetric analysis (TGA), differential thermal analysis (DTA), and energy-dispersive X-ray (EDX).

Synthesis of copper nanoparticles via chemical reduction method

Methods earlier used by [1], [36] and [37] were adopted for this work with slight modification. In a green synthetic procedure, CuCtsNPs were obtained *via* a wet chemical reduction route. 0.1 M $CuSO_4.5H_2O$ aqueous solution was prepared and 50 mL of the aqueous solution was transferred into a 500 mL conical flask. 100 mL of 3% chitosan solution was added changing the colour from blue to light blue indicating copper chitosan complex. The mixture was heated using a hot plate with

magnetic stirring at a temperature of 100 °C. After 30 min, 25 mL of 0.2 M L-ascorbic acid solution was added drop wise into the flask while stirring and the light blue colour changed to white. With the passage of time, the colour dispersion gradually changed from white, orange, brown and finally dark brown with a number of intermediate stages. The appearance of orange colour indicates the formation of fine nanoscale copper chitosan particles from L-ascorbic acid assisted reduction. The resulting dispersion was allowed to cool and was centrifuged at 2000 rpm for 40 min. The supernatant was decanted and the particles obtained were washed thrice using distilled water to ensure purity. The washed nanoparticles were oven dried at 40 °C for 24 h, pulverised into fine powder and properly stored in a desiccator devoid of light for further use.

Synthesis of 2,4-D dimethylamine herbicide onto CuCtsNPs

The encapsulation of 2,4-D dimethylamine herbicide onto CuCtsNPs was done in-situ using method described by [12]. 50 mL of 0.1 M $CuSO_4.5H_2O$ aqueous solution was transferred into a conical flask. 100 mL of 3% chitosan solution was added changing the colour from blue to light blue. After 30 min stirring, 25 mL of 0.2 M L-ascorbic acid solution was added drop wise into the flask and 360 ppm of 2,4-D herbicide formulation was added to the stirring mixture as soon as the brown colour appeared and was heated for 2 h. The resultant mixture was allowed to cool down and doubled centrifuged at 2,000 rpm for 40 min and supernatant was collected and analyzed for the amount of unloaded or free a.i in the mixture while the particles were washed thrice using distilled water and oven dried at 40 °C for 24 h. The dried nanoparticles were grounded into fine powder, stored in an air tight sample vial and kept in a vacuum desiccator devoid of light for further use and characterization.

Swelling capacity of the synthesized CuCtsNPs and 2,4-D-CuCtsNPs

To evaluate the swelling capacity of the CuCtsNPs and 2,4-D-CuCtsNPs, method according to [38] was adopted in this study. 0.5 g of the synthesized nanoparticles was immersed in 10 mL of potassium dihydrogen orthophosphate buffer solution (pH 7.0) at an ambient temperature. Excess buffer on the surface was removed with the aid of filter paper, the weight of the swollen sample was taken at various time intervals. The process was repeated at different time interval until no further weight gain. The swelling capacity was calculated using the following equation:

$$Swelling\ capacity\ (SI) = \frac{Wa - Wb}{Wb} \quad (1)$$

where, $Wa$and Wb represent the weight of swollen and dry NPs, respectively.

Characterization of synthesized and encapsulated CuCtsNPs

Formation of the CuCtsNPs and 2,4-D-CuCtsNPs was monitored using UV-Visible spectrophotometer (Cary 300 UV-Visible spectrophotometer, software version 4.20). The spectrophotometer baseline correction was done using distilled water (blank). The particle size distribution and morphology of the synthesized and loaded CuCtsNPs was done using high resolution transmission electron microscope (HR-TEM) TF 20 Tecnai $G^2$200kV (FEI) with field emission gun (FEG) working at an acceleration voltage of 200 kV and SEM (Tescan, model VEGA3) operated at accelerating voltage of 15 kV. The possible molecular interaction (s) between the synthesized and loaded CuCtsNPs was carried

out using an FT-IR instrument (Shimadzu FTIR-8400 S FT-IR spectrophotometer) and scanning was carried out and recorded within the range of 4000-400 cm^{-1}, with 2 cm^{-1} resolution and 10 scans. X-ray diffraction patterns were obtained for the synthesized and loaded CuCtsNPs using PANalytical X'Pert PRO diffractometer operated at 40 kV and 30 mA with Cu-Kα radiation (λ=1.5406). Working conditions used include 2θ scanning range of 5.0-80.0°, scanning step size of 0.02, speed of 1.00 s, sample length of 10.00 mm and measurement temperature of 25 °C. Thermal characterization of the nanoparticles was carried out using a TGA instrument (PerkinElmer TGA 4000 thermogravimetric analyser) with operating condition of heating from 30 °C-950 °C at 10.00 °C/min. DSC characterization was carried out for the synthesized and loaded CuCtsNPs using a DSC instrument (Mettler STAR^e SW 13.00 differential scanning calorimeter) with a heating rate of 10.00 °C min^$^{-1}$ over a temperature range of 30-310 °C with 34.98 °C left limit and 300.21 °C right limit in an ambient air. The elemental composition for the synthesized and loaded CuCtsNPs was carried out using ESEM coupled with EDX.

Preparation of 2,4-D stock solution and calibration curve

2,4-D stock solution was prepared using analytical grade of 2,4-D (PESTANAL®). To prepared 250 mg/L, 250 mg of 2,4-D (analytical grade) was dissolved in a beaker, transferred into a 1000 mL volumetric flask and was made to mark with distilled water. Six point serial dilutions (20, 40, 60, 80, 100 and 120 ppm) of the herbicide were prepared from its stock solutions as working standards. Absorption readings for 2,4-D were scanned from 215-325 nm to obtain the absorbance maximum at 300 nm and a standard calibration curve was obtained by plotting concentration verses absorbance, as shown in Figure 1.

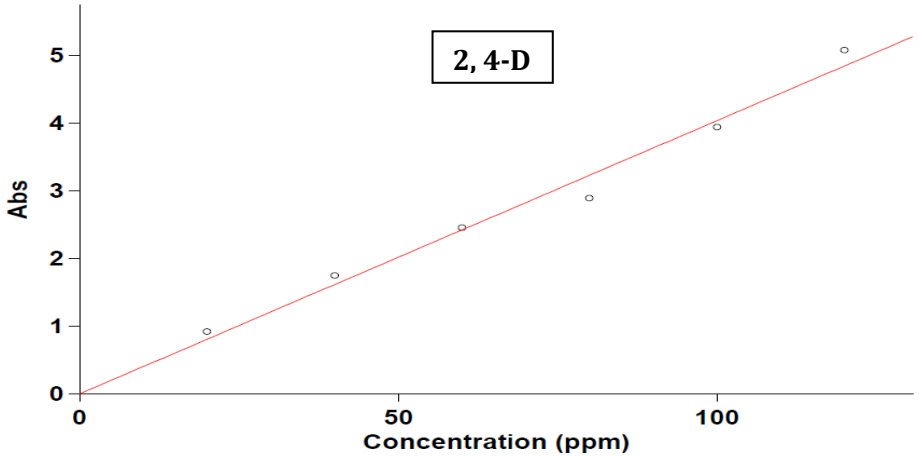

Figure 1. Standard calibration curve for 2,4-D at 300 nm

Aqueous release studies of 2,4-D-CuCtsNPs

Methods earlier reported by [12] and [1] were adopted for the release study in water. 0.5 g of 2,4-D-CuCtsNPs was placed in a 15 mL vial at ambient temperature. The mixture was shaken and at definite time intervals, 3 mL of dissolution medium was withdrawn and then replaced with fresh solution to maintain sink condition. The time intervals ran from 0, 0.1,

0.3, 1, 2, 3, 4, 5, 6, 12, 24, 48, 72 hours through 20 days. The withdrawn samples were analyzed by means of UV-Vis spectrophotometer for the amount of a.i released. Concentration of herbicide released from nano-matrix was calculated from the calibration plot of 2,4-D.

Effect of pH on aqueous release of 2,4-D-CuCtsNPs

The effect of pH on the release patterns were studied for the formulated nano-2,4-D herbicide using different (pH 5.5, 7.0 and 8.0) media to monitor the release process at ambient temperature for 14 days. The absorbance of the resultant solution was measured with the aid of UV-Visible spectrophotometer.

Aqueous release of 2,4-D-CuCtsNPs in soils

Soil leaching experiment was performed using leaching columns to study the leaching potential of released a.i from both free and encapsulated 2,4-D-CuCtsNPs. Procedure earlier stated by [39] was used with slight modifications. The soil column tubes of 2.5 mm thick inner diameter and 15 cm long were packed with glass wool to a height of approximately 4 cm at the bottom to keep the soil, prevent losses and contamination of the leachates with the soil particles. 5 g of the untreated air-dried and 2 mm sieved soils were manually packed into the glass columns upto10 cm with spatula under gentle column vibration until no further sinking of the soil to obtain uniform packing for reproducible results. The packed columns were pre-wetted with 15 mL of the artificial rain (0.01 M $CaCl_2$ aqueous solution) from top to bottom to displace available air in the soil pores by water. The columns were allowed to equilibrate and excess water was drained off. 0.5 g 2,4-D-CuCtsNPs was weighed and applied evenly over the surface of the wet soil in the columns (Figure 2). The columns were leached with 5 mL of the artificial rain drop-wise with the aid of an adjustable 25 mL burette to mimic rain drop and to control the velocity of water flux. The leachate was collected into a fitted flat-bottom flask and transferred into a 5 mL sample vial. The soil column leaching experiments were carried out for 10 days to represent 10 successful rainfalls. The leachates collected daily from the soil columns were analyzed using UV-Visible spectrophotometer.

Results and Discussion

Synthesis of the CuNPs *via* a wet chemical reduction route was followed by a series of colour change ranging from light blue, white, orange, brown and finally dark brown with a number of intermediate stages as shown in Plate 1. During the synthesis, 0.1 M aqueous $CuSO_4.5H_2O$ was added to 3% Cts solution to give a light blue colour change (Plate 1) indicating the formation of CuCts complex [Cu(Cts)] which is in agreement with the work of [40]. The light blue colour changed to white on adding 0.2 M L-ascorbic acid in drop under magnetic stirring. The appearance of orange colour in the process indicated the formation of nanoscale CuNPs from L-ascorbic acid assisted reduction. The observation here was in good agreement with previous work carried out by [37]. The formation of colours in reaction solutions observed in this study arises from the excitation of surface Plasmon vibration in the metal nanoparticles [41, 42].

The green wet chemical reduction route employed for this study, chitosan acts as capping and stabilizing agent because of its ability to chelate metal [43, 44] owing to the presence of OH groups and highly reactive amino groups [34] which help in prevent agglomeration common to CuNPs [35]. L-ascorbic acid functions as an antioxidant and a reducing agent to avoid oxidation. The

antioxidant properties came as a result of its ability to scavenge free radicals and reactive oxygen molecules [37]. The choice of $CuSO_4.5H_2O$ as precursor for this study was based on its easily oxidisable nature which enhances nanoscale structures [45].

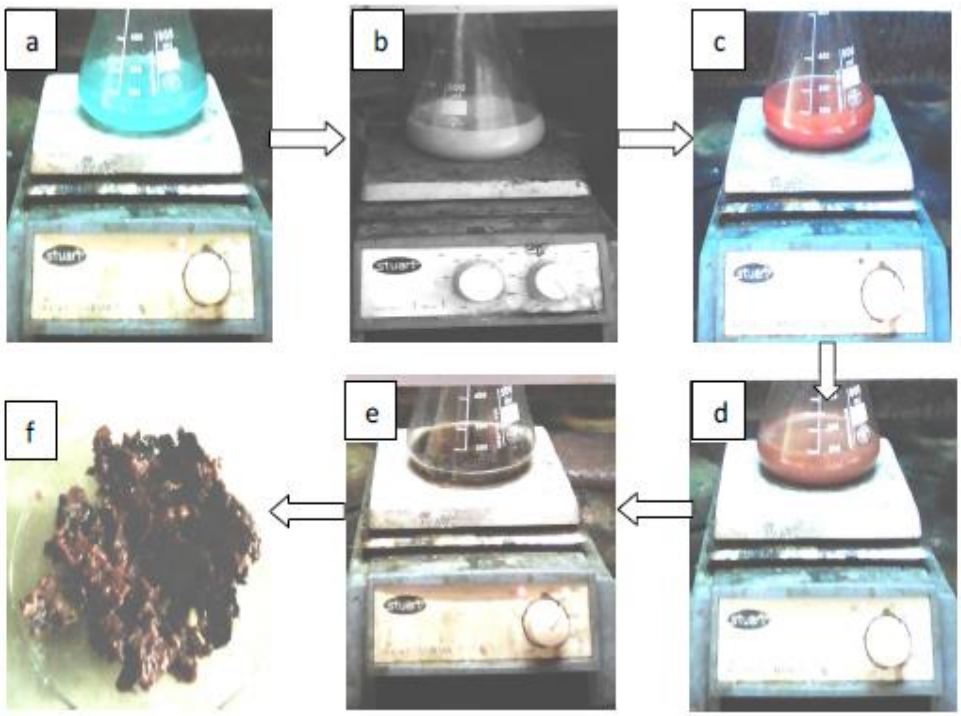

Figure 2. Step-wise synthesis of CuCtsNPs indicating color variation

Swelling capacity (index) of CuCtsNPs

The swelling behavior for the synthesized and 2,4-D loaded CuCtsNPs were carried out in a neutral environment (pH 7.0) at different timing (10, 20, 30, 40, 50 through 120 min). The swelling capacity of a material is an important property to be determined in hydrophilic polymer to enable its usage in controlled delivery systems as it correlates with diffusion rate of the penetrating solvent into the matrix and the release behavior. This property aid its use as a biomaterial in agriculture, medicine and the likes [46, 47]. The swelling ability of polymeric nanoparticles is greatly dependent on the nature of the polymer and the solvent used [38]. The swelling capacity of the synthesized and 2,4-D loaded CuCtsNPs with respect to time was presented in Figure 3 and the particles shows a steady increase in its weight as a result of it surface permeability until a constant weight was reached indicating the surface saturation [39, 48, 49].

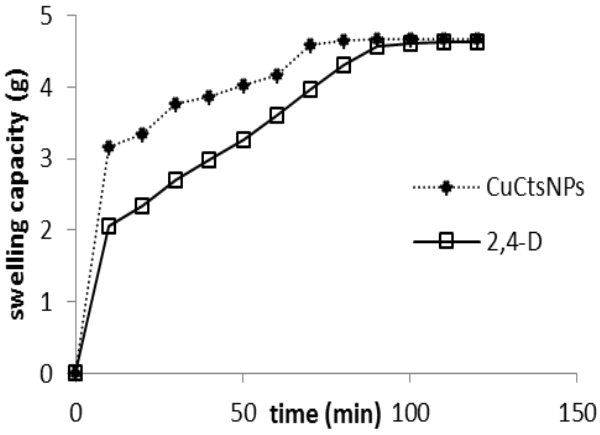

Figure 3. Swelling capacity for CuCtsNPs and 2,4-D-CuCtsNPs

UV-Visible spectrophotometric analysis of CuCtsNPs and 2,4-D-CuCtsNPs

UV-Visible spectrophotometric analysis is an important technique that is very useful in studying metal nanoparticles since shapes and peak position are sensitive to particle size. Researches carried out by other authors have reported decreasing size of metallic nanoparticles as a result in the blue shift of their surface plasmon resonance (SPR) and copper nanoparticles usually exhibit SPR around 500-600 nm [50, 37]. The synthesized CuCtsNPs and 2,4-D-CuCtsNPsshowed a characteristic absorption peak at 560 nm and 558 nm respectively as shown in Figure 4 which was almost similar to the 567 nm obtained by [51]. This absorption value indicates the reduction of Cu^{2+} ions in the presence of chitosan and the use of L-ascorbic acid as reducing agent leads to the formation of well-defined and highly monodisperse nanoparticles [52, 44]. The electron-rich oxygen atoms of polar hydroxyl groups of the chitosan are most likely to interact with electropositive metal cations [44] and the in process acts as a stabilizer as well as control nucleation [53]. The characteristic maximum absorption band observed in this work for 2, 4-D-CuCtsNPs proves it falls within the accepted range [53, 35].

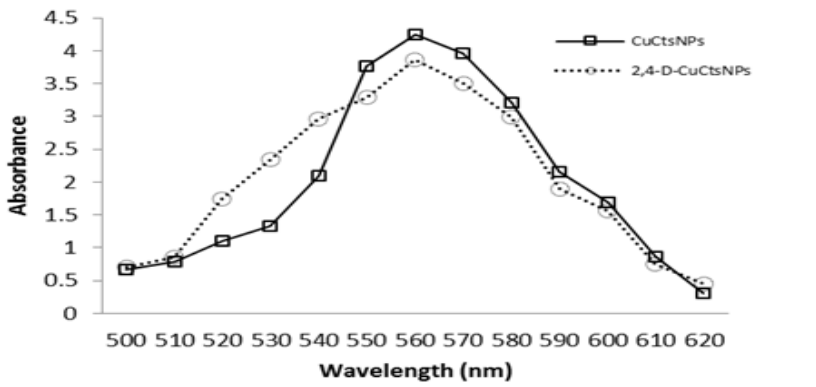

Figure 4. Absorption maxima for the synthesized CuCtsNPs and 2,4-D-CuCtsNPs

Transmission electron microscopic analysis

Transmission electron microscopy (TEM) is a technique widely employed to study the size, shape and morphology of nanoparticles using imaging, crystallographic and phase orientation information through diffraction patterns that enables the discovering of chemical composition of the particles via the energy spectrum [55]. TEM images were obtained for the synthesized and loaded CuCtsNPs using HR-TEM as shown in Figure 5 and 6. The shape obtained from the TEM micrograph were observed to be spherical which confirms the formation of monodispersed spherical CuCtsNPs, though some aggregates were seen. Similar shapes were observed from previous work carried out by [55] and [51]. The particle sizes estimated were in the range of 2-10 nm which were smaller to that obtained from the XRD pattern. The results obtained in this study agree with works of other authors [35, 51, 55, 58]. The selected area electron diffraction (SAED) shows that the synthesized nanoparticles were a collection of a large number of crystals showing different orientations as indicated by individual reflections within the rings.

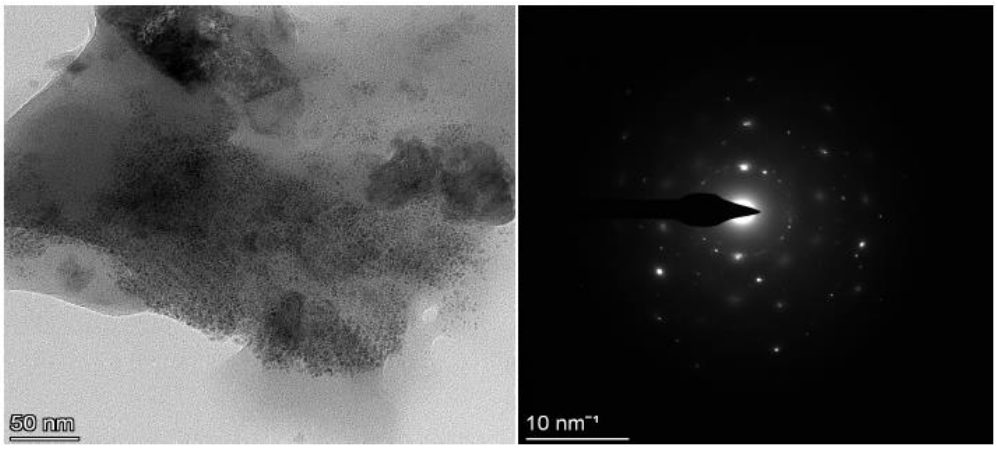

Figure 5. TEM image and SAED for the synthesized CuCtsNPs

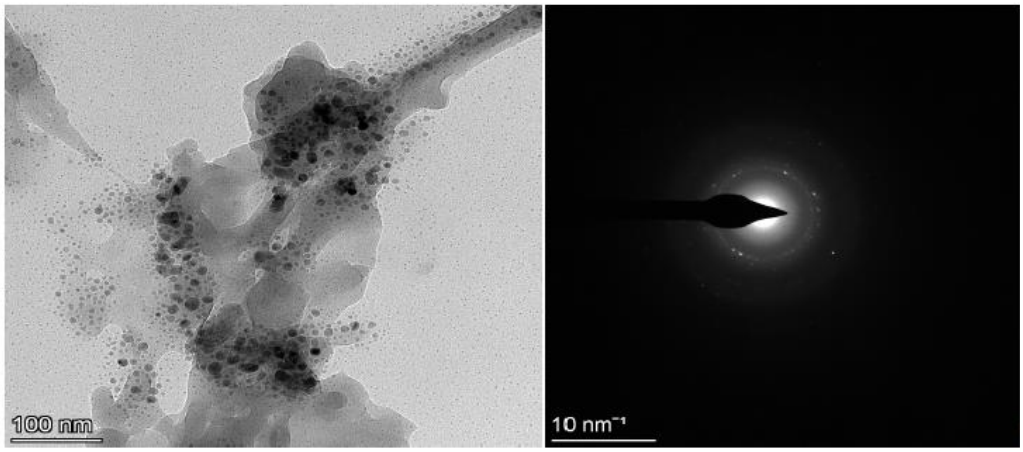

Figure 6. TEM image and SAED for the formulated 2,4-D-CuCtsNPs

Scanning electron microscopic analysis

The synthesized nanoparticles were subjected to SEM analysis to study the surface morphology of the particles using Tescan SEM VEGA3. The obtained images for the synthesized and loaded CuCtsNPs were presented in Figure 7 and 8. The image indicates clearly that the particle size obtained CuCtsNPs were small with size ranging from 21-56 nm and mostly spherical in shape [54, 55]. The image obtained for 2,4-D-CuCtsNPs, indicates clearly that the particle size obtained were small with size ranging from 25-69 nm and show shapes ranging from rod to bud-shape [56, 45, 54, 55]. The particle sizes obtained in this study were almost similar to those obtained by other authors [57, 55, 58].

Fourier transforms infrared spectrophotometric analysis

The synthesized nanoparticles were subjected to FT-IR spectrophotometric technique to determine the molecular interaction (s) between L-ascorbic acid, chitosan, the synthesized CuCtsNPs and the 2,4-D loaded CuCtsNPs as were presented in Figure 9 and interpreted in Table 1.

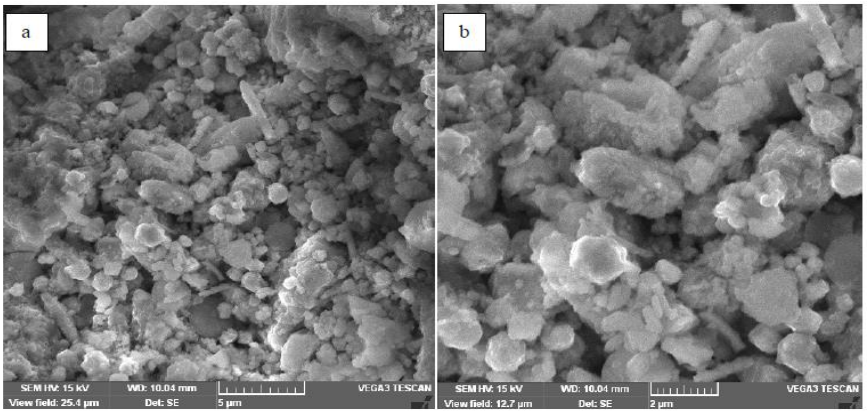

Figure 7. SEM image for the synthesised CuCtsNPs at a) 5,000 and b) 10,000 magnification

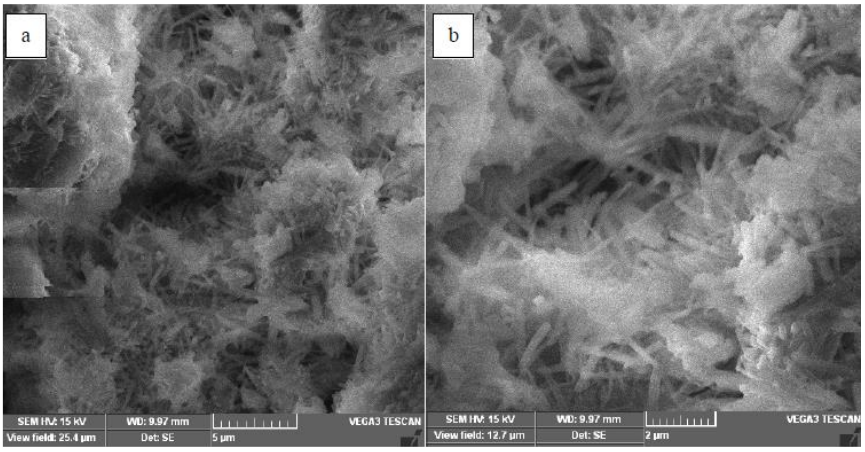

Figure 8. SEM image for the formulated 2,4-D-CuCtsNPs a) 5,000 and b) 10,000 magnification

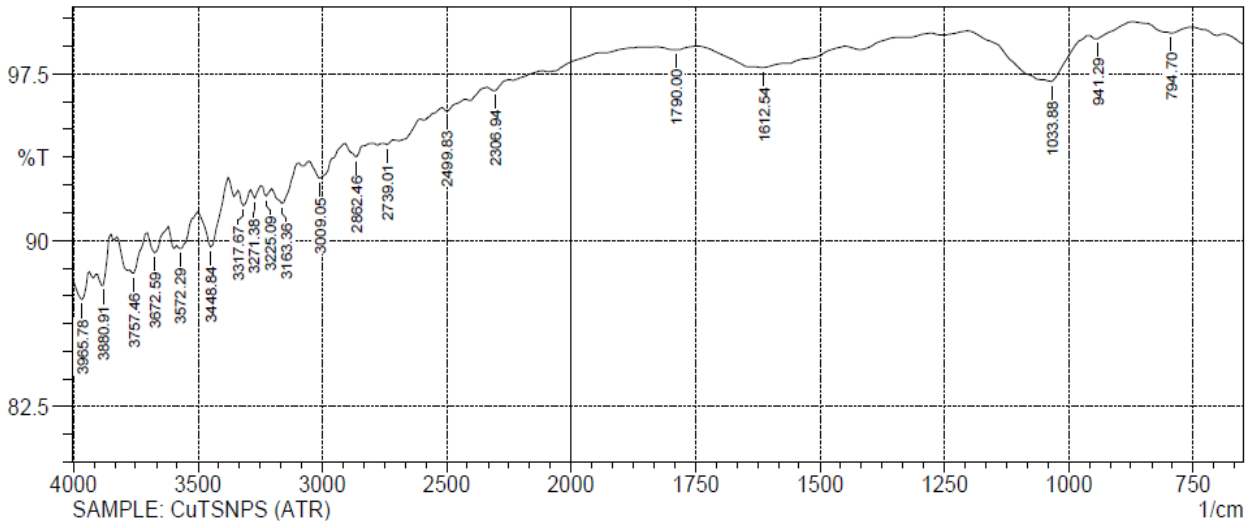

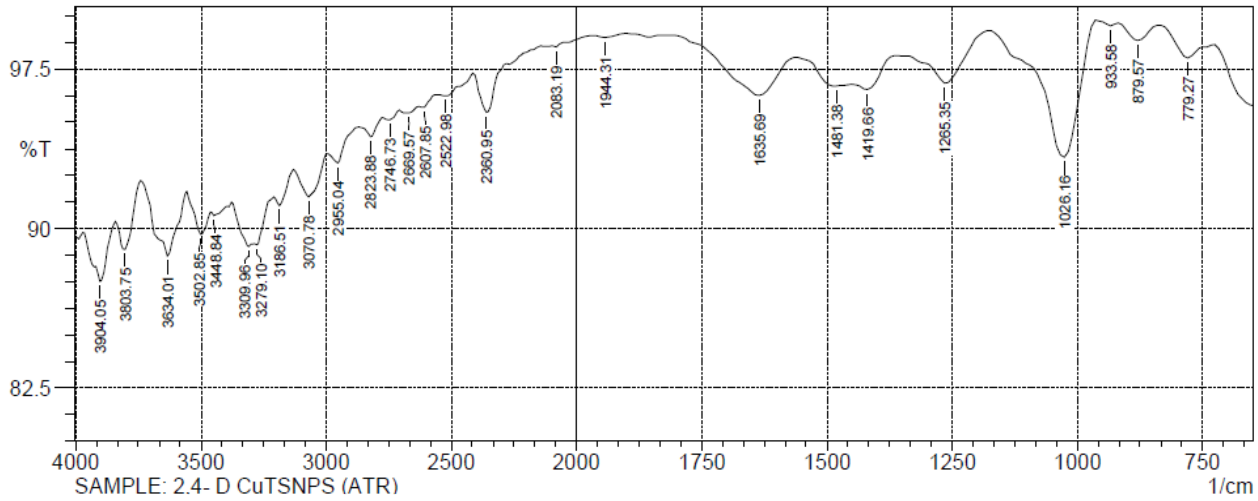

Figure 9. FT-IR spectrum for the synthesized CuCtsNPs and 2,4-D-CuCtsNPs

Table 1. FT–IR functional group analysis for CuCtsNPs and 2,4-D-CuCtsNPs

Group frequencies (cm^{-1})	Functional group	Observed frequencies (cm^{-1}) for; CuCtsNPs	2,4-D-CuCtsNPs	Vibration assignment
3750 -3500	O – H	3572 (s, b)	3503 (m)	Hydroxyl group, H-bonded OH stretch
3570 - 3200	N – H, O – H	3449 (s, b)	3310 (s, b)	Amine, hydroxyl overlap
3300 - 2900	N – H	3163, 3009 (m)	3071 (w-m)	Amine stretch
3000 - 2700	C – H	2862 (m)	-	Aliphatic C-H stretch
1900 - 1650	C = O	1790 (s)	-	Carboxylic acid stretch
1680 - 1620	C = C	-	1636 (m)	Alkenyl C=C stretch
1420 - 1410	C – H	-	1420 (m)	Vinyl C-H in-plane bend
1300 - 1200	C – O	-	1265	Phenol CO stretch
1090 -1020	C – N, C – O	1034 (s, b)	1026 (m)	Primary mine CN, carbonyl CO stretch
900 – 860	C – Cl	-	880 (s)	1, 3-disubstituted
800 – 700	C - Cl	-	779 (s)	Chloro compound C-Cl stretch

The spectrum obtained for CuCtsNPs and formulated 2,4-D-CuCtsNPs shows absorption peak at 3572 cm^{-1}, 3634 cm^{-1} and 3503 cm^{-1} were due to the presence of intramolecular H-bonds stretch and corresponds to free phenolic hydroxyl group [59]. This indicates that the encapsulation of 2,4-D-CuCtsNPs unto the synthesized CuCtsNPs was successful [37, 59]. The peaks at 3449 cm^{-1}, 3310 cm^{-1}, 3071 cm^{-1}, 1790 and 1613 cm^{-1} corresponds to amino groups, oxidized ester carbonyl and a conjugated carbonyl group respectively. These results indicate the presence of oxygen availability on the surface of the CuCtsNPs obtained from chitosan and L-ascorbic acid [40, 51, 37]. This shows that L-ascorbic acid plays double role in the synthesis of CuCtsNPs as an antioxidant and an excellent reducing agent [37, 59]. The peak at 2862 cm^{-1} corresponds to aliphatic C–H stretch in alkanes. The peak

observed at 1034 cm^{-1} corresponds to C–O and C–N stretch while the peak at 795 cm^{-1} indicates the interaction between CuNPs and Cts. This shows that the capping of CuNPs was carried out successfully using chitosan [35, 40]. The peak at 1636 cm^{-1} corresponds to a stretching vibration of an alkenyl C=C group [41] probably as a result of a conjugated carbonyl group. The shift observed in the wave number here (1613-1636 cm^{-1}) was due to the C=C stretch and it shows possible co-ordination with the CuNPs [37, 40, 51]. The absorption band at 1420 cm^{-1} and 1265 cm^{-1} corresponds to a vinyl C–H in-plane bend and a phenolic C–O stretch respectively. The observed peaks at observed at 880 cm^{-1} and 779 cm^{-1} corresponds a 1,3-disubstition associated with C-Cl stretch of halo compounds [60]. Thus, the formulated 2,4-D-CuCtsNPs retained it chemical composition and that of the CuCtsNPs.

Powder X-ray diffraction pattern of CuCtsNPs and 2,4-D-CuCtsNPs

The synthesized CuCtsNPs and 2,4-D-CuCtsNPs were further characterized to study its crystalline structure and phase composition. The diffractograms obtained were shown in Figure 10 and 11. Prominent diffraction peaks were observed for copper around 2θ values of 43.63°, 50.78° and 74.42° corresponding to (111), (200) and (220) crystallographic planes of face-centered cubic (fcc) copper respectively while that for 2,4-D-CuCtsNPs was around 2θ values of 43.40°, 50.52° and 74.18° corresponding to (111), (200) and (220) crystallographic planes of face-centered cubic (fcc) copper respectively. This confirms the cubic lattice of copper [58, 55, 61]. The small diffraction peak observed at 2θ value of 28.88° corresponds to (100) probably may be coming from either capping or reducing agent used. All the diffraction peaks obtained in this work (Table 2) were in good agreement with the standard pattern for pure fcc phase of CuNPs JCPDS No. 04-0836 and copper X-ray diffraction reference No. 01-089-2838 [61, 40, 45, 54, 62]. The highest intense peak for fcc material is generally observed at (111) reflection and this was observed in the synthesized CuCtsNPs. This peak indicates highly crystalline nature of the synthesized product. The significant broadening of the peaks was attributed to the nanocrystalline nature of the particles. This was evident from the size obtained using the Debye-Scherrer's equation with an average crystalline size of 38.78 nm (CuCtsNPs) and 55 nm (2,4-D-CuCtsNPs) (Table 3) [63]. This value was in agreement with the work of [57]. The 38.78 nm and 55 nm crystalline sizes indicate high surface to volume ratio and surface charge [45, 62, 10].

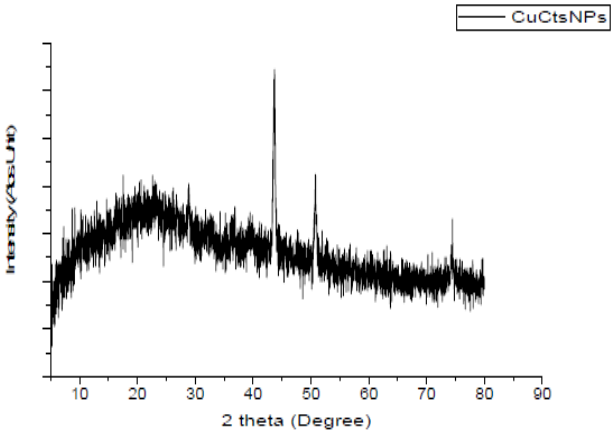

Figure 10. XRD pattern for the synthesized CuCtsNPs

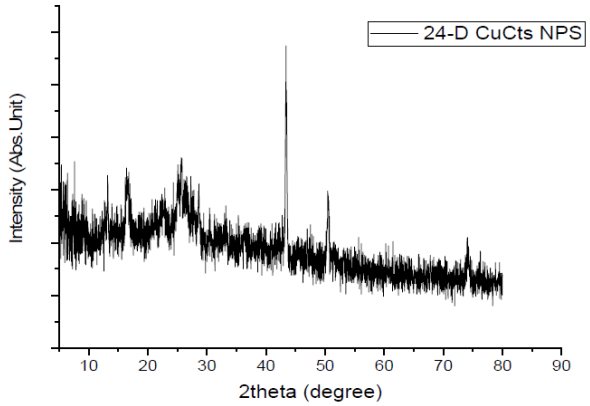

Figure 11. XRD pattern for the formulated 2,4-D-CuCtsNPs

Table 2. XRD profile information for the synthesized CuCtsNPs

Position [°2Th]	Height (cts)	FWHM [°2Th]	Crystalline size (nm)	hkl values	d-spacing (Å)	Rel. int (%)
28.88	39.96	0.4723	34.72	100	3.0920	24.42
43.63	163.64	0.3936	43.46	111	2.0746	100.00
50.78	75.06	0.3149	55.82	200	1.7977	45.87
74.42	28.42	0.9446	21.12	220	1.2748	17.37
Average crystalline size = 38.78 nm						

cts = counts, FWHM = full width at half maximum, hkl = miller indices and Rel. int= relative intensity

Table 3. XRD profile information for the formulated 2,4-D-CuCtsNPs

Position [°2Th]	Height (cts)	FWHM [°2Th]	Crystalline size (nm)	hkl values	d-spacing (Å)	Rel. int (%)
13.25	47.21	0.2362	67.69	010	6.6834	26.81
16.47	48.74	0.6298	25.48	020	5.3834	27.69
25.69	71.75	0.2362	68.97	100	3.4684	40.75
28.63	46.73	0.3149	52.05	100	3.1185	26.54
43.40	176.05	0.2362	72.37	111	2.0852	100.00
50.52	65.77	0.3149	55.77	200	1.8067	37.36
74.18	34.27	0.4723	42.16	220	1.2784	19.47
Average crystalline size = 54.93 nm						

cts=counts, FWHM=full width at half maximum, hkl=miller indices and Rel. int=relative intensity

Differential scanning calorimetric analysis of CuCtsNPs

The isothermal behavior of the synthesized CuCtsNPs and 2,4-D-CuCtsNPs was investigated using DSC technique at a heating rate of 10.00 °C min^{-1} over a temperature range of 30 to 310 °C with 34.98 °C left limit and 300.21 °C right limit in an ambient air. The DSC curves for synthesized particles were displayed on Figure 12. The curve obtained for CuCtsNPs shows a glass transition temperature (Tg) of 64.36 °C with an endothermic peak height of 2.91 mW resulting from the presence of an amorphous phase and a single exothermic peak responds which may be as a result of a new crystalline phase formation at 163.57 °C at an onset temperature of 158.88 °C and endset of 165.51 °C with peak height of 18.99 mW. According to [64], most cold crysallisation takes place at between 165 °C-200 °C, through the crystalline peak observed in this was between 158.88 °C–165.51 °C. The curve also shows a single endothermic peak responds corresponding to the melting of the NPs at 246.19 °C indicating that the amorphous polymer shows phase transition at an onset temperature of 178.69 °C and endset of 263.58 °C leading to a melting peak height of 19.21 mW [50]. The curve for 2, 4-D-CuCtsNPs shows a Tg at 131.89 °C resulting from increased crystallization with small step height with two broad exothermic peaks height of -5.99 mW at a temperature of 76.64 °C result from the presence of an amorphous phase and 17.95 mw at temperature of 236.30 °C leading to an inflect point at 278.81 °C and end set temperature of 296.07 °C tending to oxidation without melting. The values obtained here were lower than the one obtained by [50].

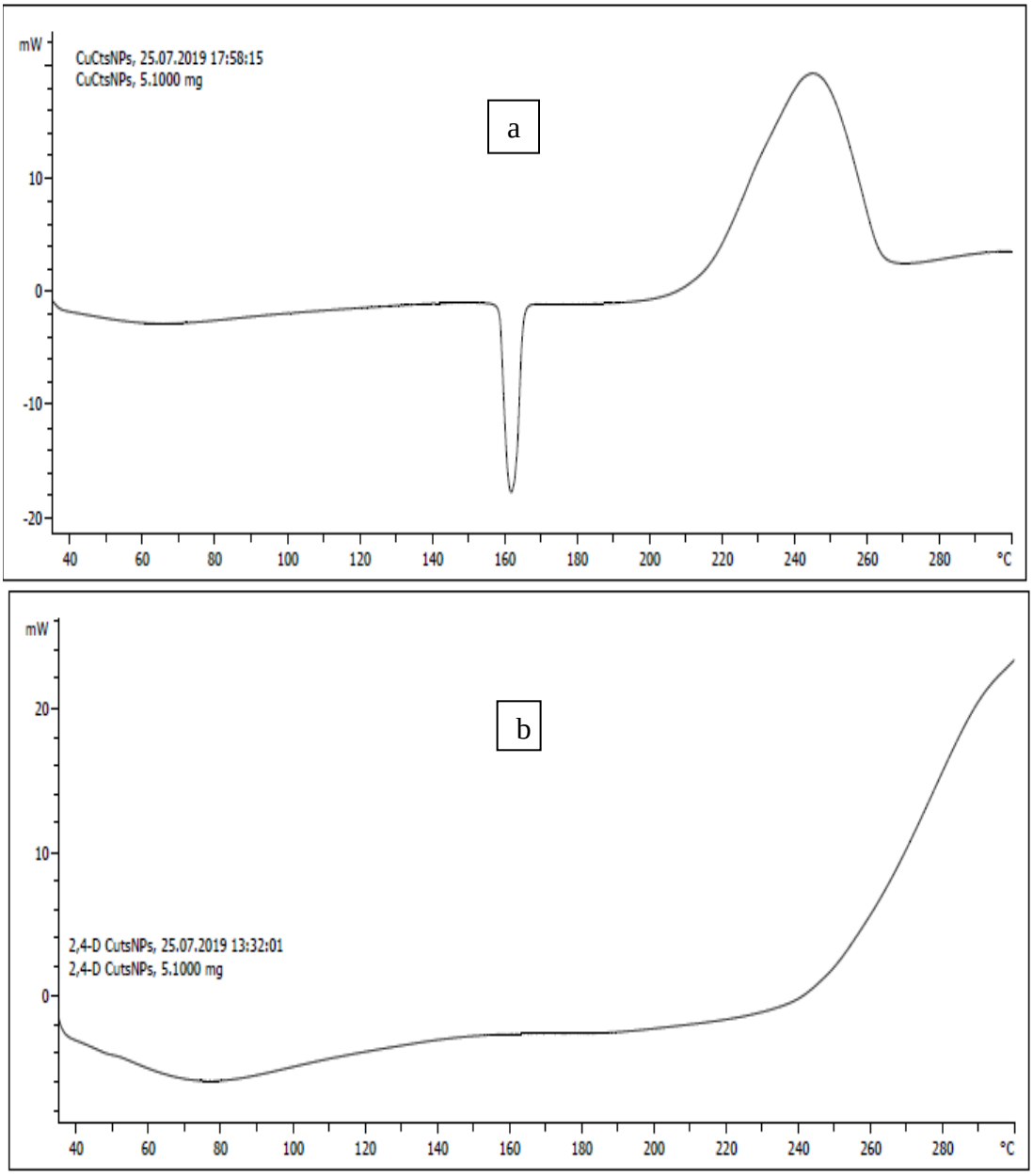

Figure 12. DSC Curve for the Synthesized a) CuCtsNPs and b) 2,4-D-CuCtsNPs.

TGA/DTA characterization of CuCtsNPs and 2,4-D-CuCtsNPs

Thermogravimetric analysis (TGA) was employed to study the thermal behavior and stability of the synthesized particles while differential thermal analysis (DTA) measures and record the temperature difference between the sample to be analyzed with a reference sample usually thermograph from TGA with operating condition of heating from 30 °C -950 °C at 10.00 °C/min. The TGA and TGA/DTA thermographs for the synthesized CuCtsNPs and 2,4-D-CuCtsNPs were shown on Figure 13. TGA curve for CuCtsNPs shows single step decomposition with initial weight loss of 11.52% from 28.13 °C to 298.69 °C due to the present of moisture and volatile matter. The decomposition of the synthesized CuNPs under

excited temperatures ranges from 28.13–298.69 °C onset, 298.69–357.90 °C midpoint and 357.90–423.76 °C complete degradation. TGA curves obtained for 2,4-D-CuCtsNPs shows three decomposition steps with initial weight loss of 2.33% from 84.71 °C to 156.55 °C was due to the present of moisture and volatile matter. The decomposition of 2,4-D-CuCtsNPs under excited temperatures ranges from 84.71–156.55 °C onset, 281.46–401.73 °C, 335.16 °C midpoint and 469.19-678.18 °C complete degradation. The gradual increase from 298.69 °C to the midpoint at 357.90 °C (42.73%) for CuCtsNPs and 281.46 °C to the midpoint at 335.16 °C (42.06%) for 2,4-D-CuCtsNPs weight losses can be linked to pyrolysis and combustion of organic compounds from the starting materials that leave the system in form CO_x (x=1, 2) [50]. The observation from this result was in line with pronounce and well resolved exothermic peak in the DTA curve at an onset temperature of 178.45 °C to 484.22 °C with maximum peak at 342.29 °C for CuCtsNPs and 258.32 °C to 436.89 °C with maximum peak at 340.08 °C for 2,4-D-CuCtsNPs. The values obtained in this study were higher than that obtained by [65] which may be due to difference in the material used for the synthesis of copper nanoparticles. The 69.90% complete degradation as observed from the curve shows that the synthesized CuCtsNPs was thermally stable up to 423.76 °C and 401.73 °C for 2,4-D-CuCtsNPs [66] (Table 4).

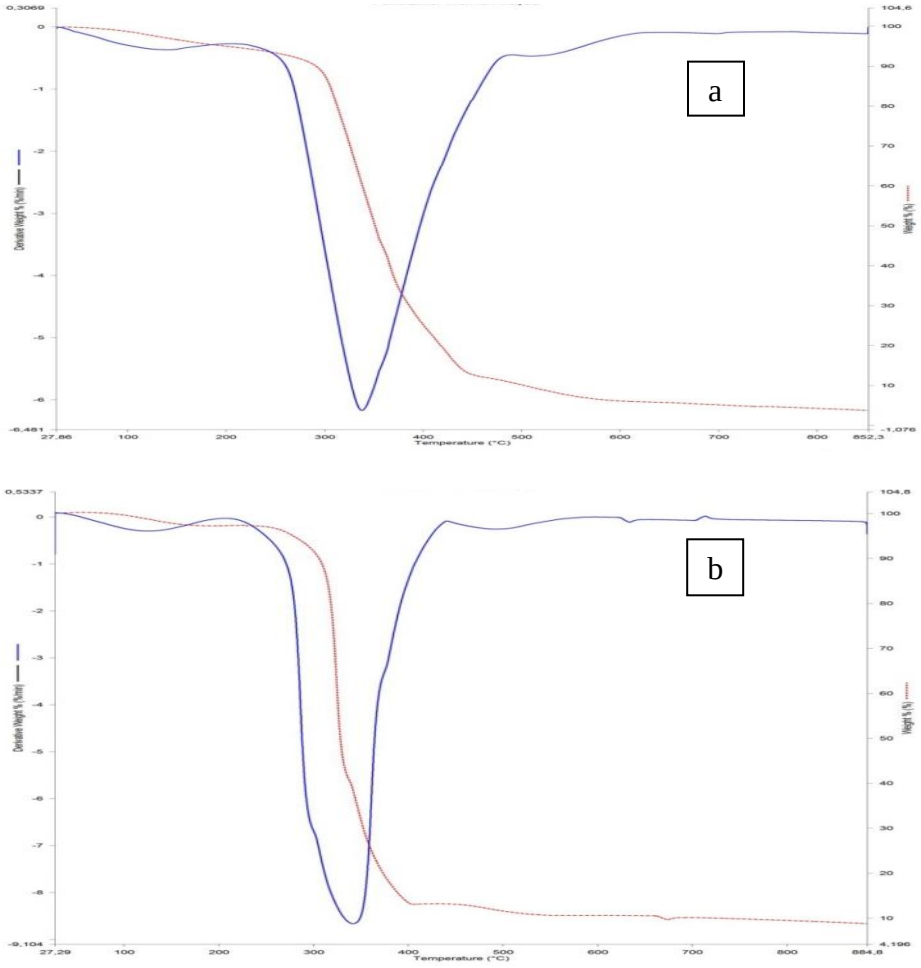

Figure 13. TGA/DTA thermograph for a) CuCtsNPs and b) 2,4-D-CuCtsNPs

Table 4. Degradation temperature and weight loss from TGA/DTA studies

Sample	Onset (°C)	Endset (°C) Wt (%)	Midpoint (°C) Wt (%)	Total Wt loss (%)	DTA Exotherm peak (°C)
CuCtsNPs	28.13 298.69	298.69 (11.52) 423.76 (69.9)	357.90 (42.73)	81.42	342.29
2, 4-D-CuCtsNPs	84.71 281.46 469.19	156.55 (2.33) 401.73 (81.42) 678.18 (2.77)	335.16 (42.06)	86.52	340.08

Energy dispersive X-ray analysis of CuCtsNPs and 2,4-D-CuCtsNPs

The synthesized nanoparticles were also characterized using EDX for elemental composition determination presented as atom percentage. The analysis was performed using ESEM coupled with EDX operating at 15.0 kV. The EDX spectrum recorded for the synthesized and loaded CuCtsNPs were shown in Figure 14. The profile shows a strong copper signal at 8 keV along with oxygen and carbon peaks, which may have originated from the biopolymer bound to the surface of the copper nanoparticles. From the EDX pattern, the atomic concentration obtained for Cu was 33.72% and the highest weight of 60.37% followed by O_2 with 18.18% weight while profile for 2,4-D-CuCtsNPs indicated the presence of Cl and Cu as the major component in formulation with atomic concentration for Cl at 47.32% and weight of 41.72% followed by Cu with 38.45%. This implies that the oxygen from either the capping or reducing agent was not lost but was able to bind to the surface of the CuNPs [54, 35].

Aqueous release studies of formulated 2,4-D-CuCtsNPs

The release process of the 2,4-D-CuCtsNPs was carried out at different time interval and the concentration of 2,4-D released in the process per time was determined from their absorbance readings. The percentage cumulative release was calculated using the initial 2,4-D concentration and the release at different time. The release of the herbicide a.i was monitored for three (3) weeks and was found to increase steadily with contact time as the release process progresses. The result obtained was shown in Figure 15. Herbicide release from nanoparticles is usually a biphasic phenomenon although in some instances a triphasic trend is observed [1]. The mode of release in aqueous medium showed a steady release pattern as the time increases. The herbicide release profile exhibited an initial burst release, presumably from the particle surface, followed by slow release driven by polymer erosion and diffusion of a.i through the polymer pore [48, 47, 12]. This can be an advantage since it can control the sprouting of weed seeds and still exist to kill and inhibit new infestation [24, 29]. Release profile for the 2,4-D-CuCtsNPs gave a reasonable, sustainable and steady release. The release of herbicide a.i from the loaded CuCtsNPs is determined basically by size of the nanoparticles, nature of reagents employed the molecular weight of the polymeric material and the type of interaction involved. Looking at different release profile in this work after three weeks (21 days) and the percent herbicide release, it shows that the release process can still continue for a longer period.

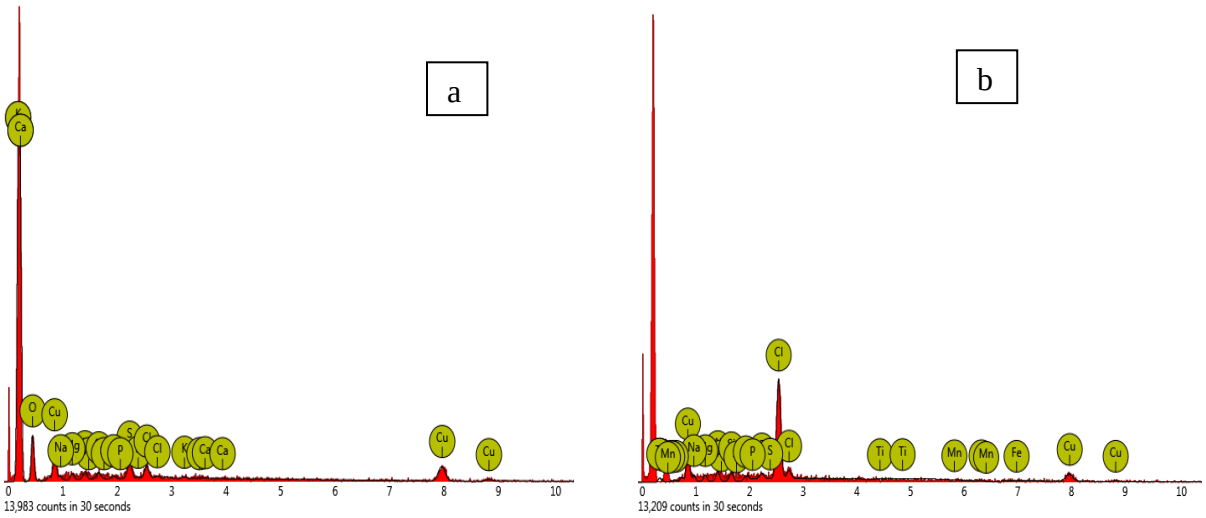

Figure 14. EDX spectrum for the synthesized a) CuCtsNPs and b) 2,4-D-CuCtsNPs

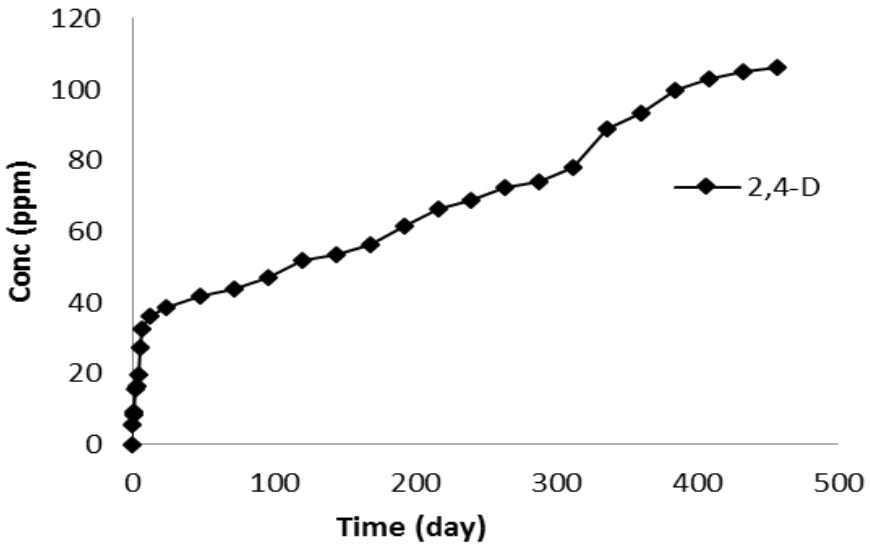

Figure 15. Aqueous release profile of 2,4-D-CuCtsNPs

Effect of pH on aqueous release of 2,4-D-CuCtsNPs

The effect of pH on the aqueous release of 2, 4-D-CuCtsNPs was monitored in three (3) different pH buffers which include acidic (pH 5.5), neutral (pH 7.0) and alkaline (pH 8.0) respectively. The effect of pH on the release was monitored for 14 days. The release profile and the percentage herbicide a.i release in the process were presented in Figures 16. The results obtained from the release of the herbicides a.i from the formulated 2,4-D-CuCtsNPs shows that the release pattern observed in the pH 5.5 (acidic medium) for 2, 4-D was high with percentage herbicide release of 64.39%. The difference observed in the release rate for 2,4-D in pH 5.5 can be linked to 2,4-D enhanced solubility being more persistent under acidic condition as reported by [14] and [16]. The release profile in the neutral medium (pH 7.0) also shows considerable percentage release for 2,4-D (62.06%) while the alkaline environment (pH 8.0) was observed to have the lowest release percentage of 9.50%.

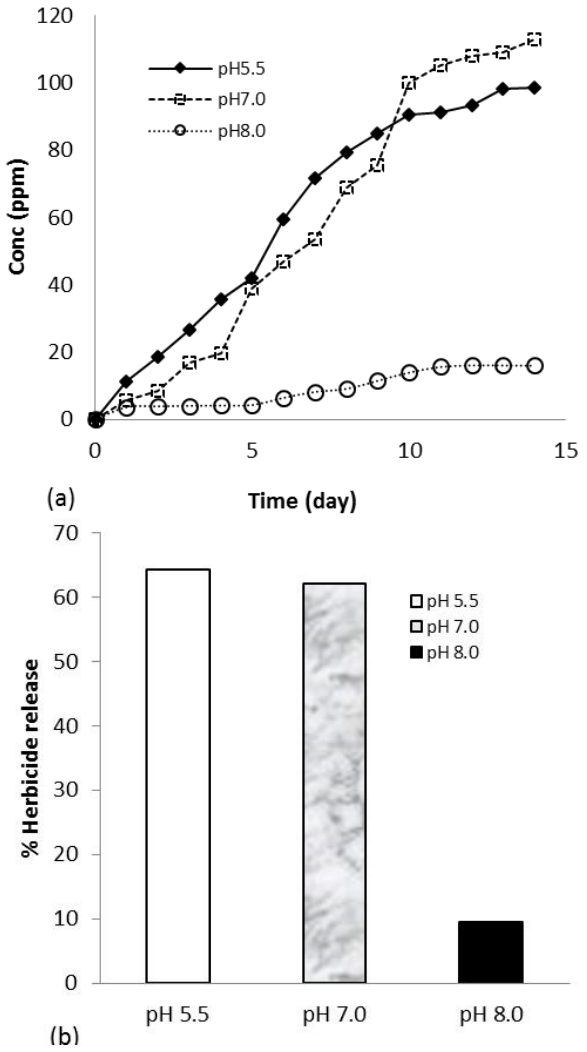

Figure 16. a) Effect of pH and b) percentage release of a.i from 2,4-D-CuCtsNPs in pH media

Aqueous release of nano-herbicide formulations using soil column

The leaching potential of the active ingredient (a.i) from both 2,4-D in soil from the synthesized CuCtsNPs were carried out using soil leaching columns of 2.5 mm thick inner diameter and 15 cm long. The leachate collected per experiment in order to mimic ten successful rainfalls was analyzed using a UV-Visible spectrophotometer. Pesticide Leaching is one of the major contaminant of groundwater and can be determined by the physicochemical properties of pesticide active ingredient, soils and rainfall. Leaching profiles of the formulated 2,4-D-CuCtsNPs through the soil layer (UAM and CAPS) were shown in Figure 17. The percentage herbicide a.i release for the herbicide in the leachate after 10 irrigations for UAM soil was higher for 2,4-D (58.67%) than the results obtained for a.i release in CAPS soil 2,4-D (40.78%). The release rate of the herbicide a.i from CuCtsNPs matrix in the two soils was slower than in water. This observation could be as a result of the soil's ability to regulate the applied artificial rain and the amount of the a.i released from the matrix which is dependent on the soil physicochemical properties. The results obtained in this study implies that encapsulating herbicides onto CuCtsNPs matrix can be a useful practice in reducing herbicide leaching in the soil as only small amount of a.i will be available for leaching. Similar observation has been reported from previous works carried out by [39] using Atrazine and Imidachloprid. The percentage herbicide profile obtained showed that the release can still continue for more time indicating that nano-formulation will be beneficial for maintaining the biological effect of herbicides for a longer time, thereby enhancing their efficiency [39].

Conclusions

This research study used green chemical reduction method to synthesize the CuCtsNPs. The study formulated an environmentally friendly herbicide delivery nano-matrix (CuCtsNPs) for the successful slow release of 2, 4-D dimethylamine herbicide in aqueous medium and agricultural soils. The method was economical, convenient, simple and effective. Both the synthesized and encapsulated CuCtsNPs were subjected to different characterization techniques including, UV-visible spectrophotometer, SEM, FT-IR, XRD, DSC, TGA, DTA and EDX in order to authenticate

the effectiveness of the synthesized nanoparticles. It was found that, the encapsulation of herbicides onto copper-polymer nanoparticles can help in reducing the negative environmental impact associated to the use of synthetic herbicides on non-target organisms, groundwater and surface waters contamination which are threatening to life and life supporting systems.

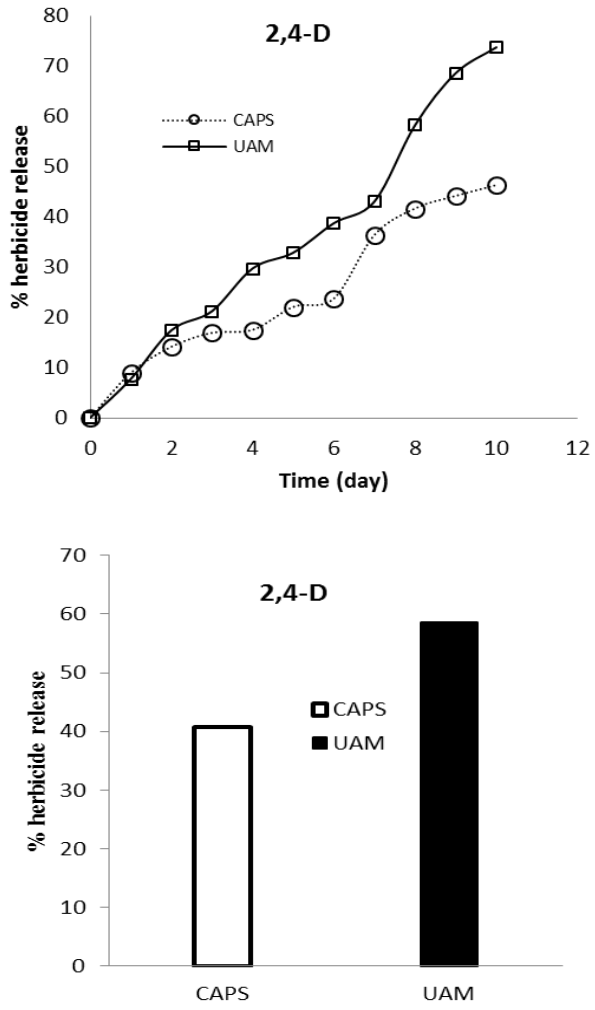

Figure 17. Percentage herbicide a.i release from 2,4-D-CuCtsNPs

Disclosure Statement

No potential conflict of interest was reported by the authors.

References

[1]. Itodo H.U., Nnamonu L.A., Wuana R.A. *A. J. Chem. Sci.,* 2017, **2**:1

[2]. Zahid H., Khan B.M., Fazal M., Abdul S., Kawsar A. *Pak. J. Bot.* 2013, **45**:55

[3]. EPA, Pesticides Industry Sales and Usage 2006 and 2007 Market Estimates. Washington (DC): Prevention, Pesticides and Toxic Substances; 2011

[4]. PRD, World Population Data Sheet: Special Focus on Youth; 2017

[5]. Sopena F., Maqueda C., Esmeralda M. *Cien. Invest. Agra.,* 2009, **35**:27

[6]. Ramadass M., Thiagarajan P. *Mater. Sci. Eng.,* 2017, **263:**1

[7]. Tornisielo V.L., Rafael G.B., Paulo A.A., Eloana J.B., Sergio H.M. *Andrew Price*, 2013, pp. 474

[8]. Dhillon N.K., Mukhopadhyay S.S. *J. Crop and Weed*, 2015, **11**:187

[9]. Nnamonu L.A., Sha'ato R., Onyido I. *Mater. Sci. Appl*., 2012, **3**:566

[10]. Choudhary R.C., Kumaraswamy R.V., Sarita K., Sharma S.S., Ajay P., Ramesh R., Pratim B., Vinod S. *Sci.Reports*., 2017, **7**:1

[11]. Grillo R., Pereira A.E.S., Nishisaka C.S., Lima R., Oehlke K., Greiner R., Fraceto L.F. *J.Hazard Mater.*, 2011, **186:**1645

[12]. Faria D.M., Sidney M.D.J., Joao P.L., Eloiza da Silva N., Renata P.M., Luciana S.R.,Jeferson, A.M. *Mater. Research,* 2017, **20**:225

[13]. Burns C.J., Swaen G.M. *Critical Rev. Toxicol.*, 2012, **42**:768

[14]. European Food Safety Authority, *EFSA J.*, 2014, **12**:7

[15]. APVMA, Annex to the APVMA's Preliminary Review Findings (Environment) Part 1: 2,4-D Esters, 2013, **1**:31

[16]. Qurratu A., Reehan A. *Int. J. of Appl. Eng. Res*., 2016, **11**:9946

[17]. GrossmannK. *Pest Mgt. Sci*. 2009, **66**:113

[18]. Song Y. *J. Integrative Plant Biol*., 2014, **56**:106

[19]. Neumeister L. The risks of the Herbicide 2,4-D, 2014; Frohschammerstr. p.12
[20]. Mcmanus S.L., Moloney M., Richards K.G., Coxon C.E., Danaher M. *Molecules*., 2014, **19**:20627
[21]. Rana S.S., Rana M.C., Advances in Weed Management, 2015; Palampur. p. 21
[22]. Maruyama C.R., Mariana G., Monica P., Natalia B., Abhilash P.C., Leonardo F.F., De Lima R. *Sci. Reports*, 2016, **6**:1
[23]. Abigail E.A., Chidambaram R. Andrew Price, 2017, pp. 207
[24]. Onyido I., Sha'Ato R., Nnamonu L.A. *J. Environ. Protection,* 2012, **3**:1085
[25]. Roy A., Sunil K.S., Jaya B., Anil K.B. *Cent.Euro. J. Chem.,* 2014, **12**:453
[26]. Shikha J., Ankita J., Vijay D. *Int. J. Sci. Eng. Res.*, 2014, **5**:973
[27]. Hassan H., Ehtesham M.Z., Rabee P., Payman R. *Int. J. Phy. Sci.,* 2011, **6**:4331
[28]. Rajesh M. *Int. Adv. Res. J. Sci. Eng. Technol*., 2016, **3**:37
[29]. Grillo R., Rosa A.H., Fraceto F.L. *Int. J. Environ. Sci. Technol.*, 2014, **11**:1691
[30]. Pereira J.R., Duarte A.E., Pitombeira J.B., Da Silva M.A.P., Beltrao N.E., Barros L.M. *Int. J.Exptal Bot.,* 2013, **82**:275
[31]. Kashyap P.L., Xiang X., HeidenP. *J. Biol. Macromolecule*, 2015, **77:**36
[32]. Angham G.H. *Chem. Mater. Res*., 2013, **3**:21
[33]. Adarsh K.J., Madhu G. *Int. J. Inno. Res. Sci. Eng. Technol*., 2013, **2**:2943
[34]. Tamayo L., Manuel A., Marcelo K., Ana R., Maritza P. *Mater. Sci. Eng. C*. 2016, **69**:1391
[35]. Manikandan A., Sathiyabama M. *J. Nanomed. Nanotechnol*., 2015, **6**:251
[36]. Jihad I.A., Hatem M.B., Sepa M.M., Heba M.F., Nada R.A. *J. Bionanosci.* 2016, **10**:15
[37]. Shikha J., Ankita J., Pranav K., Vijay D. *Trans. Nonferrous Metals Soc. China,* 2015, **25**:3995
[38]. Cahyaningrum S.E., Nuniek H., Nur Q. *Indonesia J. Chem.,* 2015, **15**:16
[39]. Jianfa L., Jian Y., Yimin L., Ying, S. *J. Environ. Sci. Health,* Part B: 2012, **47**:795
[40]. Usman M.U., Mohamed E.E., Kamyar S., Norhazlin Z., Mohamed S., Nor A.I. *Int. J. Nanomed.,* 2013, **8**:4467
[41]. Khalid H., ShamailaS., Zafar N., Shamaila S. *Sci.Int-Lahore*, 2015, **27**:3085
[42]. Argueta-Figueroa L., Raul A.M.L., Rogelio J.S.V., Oscar F.O.M. *Prog. Nat. Sci.: Mater. Int.*, 2014, **24**:321
[43]. Ancona A., Sportelli M.C., Trapani A., Picca R.A., Palazzo C., Bonerba E., Mezzapesa F.P., Tantillo G., Trapani G., Cioffi N. *Mater. Lett.,* 2014, **136**:397
[44]. Zain N.M., Stapley A.G.F., Shama G. *Carbohy.Poly.*, 2014, **112**:195
[45]. Krithiga N., Jayachitra A. *Int. J. Res. Appl. Sci. Biotechnol*., 2014, **1**: 22
[46]. Chime S.A., Onunkwo G.C., Onyishi I. *Res. J. Pharm. Biol. Chem. Sci.*, 2013, **4**:97
[47]. Fernanda C.M., de Castro A.D., Evangelista R.C.,Cury, B.S.F. *A. J. Pharm. Sci*., 2014, **9**:27
[48]. Sun W., Zhang N., Li X. *Colloid Surface B*, 2012, **95**:115
[49]. Dixit N., Sheo D., Maurya B., Sagar P.S. *Indian J. Res. Pharm. Biotechnol.*, 2013,**1**:305
[50]. Mott D., Galkowski J., Wang L. *Lang.*, 2007, **23**:5740
[51]. MiaoH., Liying L., Jinchi Z., Danzhen L. *Sci. Bull*., 2015, **60**:227
[52]. Dang T.M., Le T.T., Blanc E.F., Dang M.C. *Advan. Nat. Sci.: Nanosci. Nanotechnol.,* 2011, **2**:1
[53]. Huang H., Yuan Q., Yang X. *Colloids and Surfaces B: Biointerfaces,* 2004, **39**:31
[54]. Suresh Y., Annapurna S., Bhikshamaiah G., Singh A.K. *Int. J. Sci. Eng. Res.,* 2014, **5**:156
[55]. Sagadevan S., Koteeswari P. *J. Nanomed. Res.*, 2015, **2**:00040
[56]. Ipsa S., Nayak P.L. *World J. Nano Sci. Technol.,* 2013, **2:**14
[57]. Ayesha K., Audil R., Rafia Y., Ren C.A. *Int. Nano Lett.,* 2015, **10**:1

[58]. Phul R., Kaur C., Farooq U., Ahmad T. *Mater. Sci. Eng. Int. J.*, 2018, **2**:90
[59]. Sreeja V., Jayaprabha K.N., Joy P.A. *Appl. Nanosci.*, 2015, **5**:435
[60]. Ashtaputrey S.D., Ashtaputrey P.D., Neha Y. *J. Chem. Pharm. Sci*., 2017, **10**:1288
[61]. Theivasanthi T., Alagar M. *Arch. Physics Res.*, 2010, **1**:112
[62]. Deneke S.M., Delele W.A., Mirtachew T.A. *Ethiopian J. Sci. Technol.,* 2017, **10**:209
[63]. Monshi M., Monshi M.R., Foroughi R. *World J. Nano Sci. Eng.,* 2012, **2**:154
[64]. Schick C. *Anal. Bioanal. Chem.*, 2009, **395**:1589
[65]. Nittaya T., Chaikarn L., Sukon P. *J. Nanomater.,* 2014, 5 pages
[66]. Chaudhary J., Giriraj T., Deepak K., Ajit J. *A. J. Chem.,* 2017, **29**:1492

How to cite this manuscript: Itodo Ugbede Happiness*, Raymond Wuana, Nnamonu Lami, Sha'ato Rufus. Eco-friendly 2,4-D dimethylamine herbicide delivery system using synthesized Nano-matrix. *Journal of Medicinal and Nanomaterials Chemistry*, 2(3) 2020, 167-188. DOI: 10.48309/JMNC.2020.3.2